3-2009

The Binding of Ag+ and Au+ to Ethene

Nina J. Barnett
Iowa State University

Lyudmila V. Slipchenko
Iowa State University

Mark S. Gordon
Iowa State University, mgordon@iastate.edu

The Binding of Ag+ and Au+ to Ethene

Abstract
For the reaction M+(C2H4)n−1 + C2H4 → M+(C2H4)n, where M = Ag, Au, the binding energies are predicted at the second order perturbation (MP2) and coupled cluster (CCSD(T)) levels of theory. As the basis set is systematically improved, the predicted M = Ag binding energies steadily improve, as compared to the experimental values. In fact, the complete basis set limit (CBS) predicted CCSD(T) binding energy for Ag(C2H4)+ is within experimental error. For MP2, as the basis set is improved, the agreement with experiment worsens. Gold ions are predicted to bind more strongly than silver ions to ethene ligands. Mulliken population analyses of the silver and gold systems exhibit delocalization of the positive charges of the metal ions onto the ethene ligands. Reduced variational space analysis indicates that electrostatic interactions are the principal contributor to the bonding in these systems. Multiconfigurational self-consistent field calculations do not support the Dewar−Chatt−Duncanson model of transition metal−alkene bonding in Au(C2H4)+.

Disciplines
Chemistry

The Binding of Ag^+ and Au^+ to Ethene†

Nina J. Barnett, Lyudmila V. Slipchenko, and Mark S. Gordon*

Department of Chemistry, Iowa State University, Ames, Iowa 50011

Received: January 14, 2009; Revised Manuscript Received: February 27, 2009

For the reaction $M^+(C_2H_4)_{n-1} + C_2H_4 \rightarrow M^+(C_2H_4)_n$, where M = Ag, Au, the binding energies are predicted at the second order perturbation (MP2) and coupled cluster (CCSD(T)) levels of theory. As the basis set is systematically improved, the predicted M = Ag binding energies steadily improve, as compared to the experimental values. In fact, the complete basis set limit (CBS) predicted CCSD(T) binding energy for $Ag(C_2H_4)^+$ is within experimental error. For MP2, as the basis set is improved, the agreement with experiment worsens. Gold ions are predicted to bind more strongly than silver ions to ethene ligands. Mulliken population analyses of the silver and gold systems exhibit delocalization of the positive charges of the metal ions onto the ethene ligands. Reduced variational space analysis indicates that electrostatic interactions are the principal contributor to the bonding in these systems. Multiconfigurational self-consistent field calculations do not support the Dewar−Chatt−Duncanson model of transition metal−alkene bonding in $Au(C_2H_4)^+$.

Introduction

Over the past few years it has been discovered that while condensed phase silver and gold are chemically inert, nanoscale particles of these metals have catalytic properties.[1,2] In particular, silver clusters on semiconductor surfaces catalyze the epoxidation of ethene.[1,3,4] Small gold clusters also catalyze the partial oxidation and partial hydrogenation reactions of ethene.[2] A possible first step in these reactions is the formation of silver−ethene or gold−ethene complexes.

Previous experiments and calculations have increased knowledge of Au^+ and Ag^+ bonding to alkenes and lend a fundamental understanding to catalytic processes.[1−4] Much of the experimental and theoretical exploration has been obtained for silver−propene[4] or gold−propene[2] complexes.[5] Binding energies of silver to ethene have been explored experimentally as well, but these species have not been studied as thoroughly with theoretical/computational techniques.[1]

Experimentally, the silver−ethene system has been studied and the binding energies of $Ag(C_2H_4)_n^+$ ($n = 1-6$) have been determined. Silver ions were created by a pulsed laser impinging on the surface of a silver rod; then Ag^+ ions were mass selected by a quadrupole mass filter. The selected ions were then injected into a drift cell containing 5 Torr of He and 0.1−0.5 Torr of C_2H_4. An electric field directed the products toward a second quadrupole for detection and identification. For the reaction

$$Ag^+(C_2H_4)_{n-1} + C_2H_4 \rightarrow Ag^+(C_2H_4)_n \qquad (1)$$

the binding energy was determined at several temperatures, and these data were used to calculate the 0 K binding energy for each addition of a ligand.[1]

The silver−ethene system has also been examined by Manard and co-workers[1] using density functional theory (DFT). Calculations were performed by using the B3LYP hybrid functional[6] with the 6-31+G (d,p) basis set[7] describing carbon and hydrogen, while silver was described by using a valence double-ζ basis set and a (5s6p4d)/[3s3p2d] contraction of the Hay-Wadt ($n + 1$) effective core potential (ECP).[8] These theoretical results yield binding energies that are in good agreement with the experimental values for $n = 1$, with worsening agreement for $n = 2-4$.[1]

Recently, Olson and co-workers calculated the binding energy of Ag^+ to propene to within experimental error using coupled cluster methods and newly developed correlation consistent basis sets and associated effective core potentials for Ag^+.[5,9] These methods were then used to predict the binding energy of Au^+ to propene.[5] Due to the success of these methods and basis sets, in the present work they are extended to the binding energies of $Ag(C_2H_4)_n^+$ and $Au(C_2H_4)_n^+$, $n = 1-3$. These computational predictions provide additional insight into coinage metal bonding to alkenes, as well as a theoretical benchmark for assessing the efficacy of DFT and second-order perturbation theory (MP2) calculations for predicting accurate binding energies of alkenes to these metals.

Computational Approach

Geometry optimizations of C_2H_4, $Ag(C_2H_4)_n^+$, and $Au(C_2H_4)_n^+$, $n = 1-3$, were performed with GAMESS,[10] using the 6-31G+(d) basis set for C and H.[11] Silver and gold atoms were initially described by using the SBKJC[12] effective core potential (ECP) and associated basis set, augmented with one set of f-functions for Ag (exponent = 1.30) and Au (exponent = 0.89). These ECPs include scalar relativistic corrections.

All geometry optimizations were performed at the MP2[13] level of theory. To ensure that the optimized geometries were minima on the potential energy surface (PES), Hessians (energy second derivatives) were calculated for each optimized geometry. A positive definite Hessian indicates a minimum on the potential energy surface. Especially for three ligands, an exhaustive search was carried out from various starting geometries, in order to find other minima on the potential energy surface. No additional minima were found.

Once the geometries were determined as described above, single point energies were calculated at these geometries with Molpro,[14] using correlation consistent basis sets,[15] and the cc-pVXZ-PP (X = D, T, Q) basis sets[9] developed by Peterson and

† Part of the "Robert Benny Gerber Festschrift".

* To whom correspondence should be addressed.

10.1021/jp900372d CCC: $40.75
Published on Web 03/25/2009

TABLE 1: $Ag(C_2H_4)^+$ System: Total Energies (hartrees) and Binding Energies (eV)[a]

	total energies			
	Ag^+	C_2H_4	$Ag(C_2H_4)^+$	E_B (eV)
DZ-HF	−145.82049	−78.03968	−223.89183	0.86
DZ-MP2	−146.08375	−78.31504	−224.45326	1.48
DZ-CCSD(T)	−146.07586	−78.35513	−224.48018	1.34
TZ-HF	−145.82166	−78.06320	−223.91651	0.86
TZ-MP2	−146.18204	−78.39914	−224.64032	1.61
TZ-CCSD(T)	−146.16824	−78.43877	−224.65970	1.43
QZ-HF	−145.82184	−78.06846	−223.92196	0.86
QZ-MP2	−146.22170	−78.42503	−224.70774	1.66
QZ-CCSD(T)	−146.20604	−78.46166	−224.72218	1.48
CBS-HF	−145.82187	−78.06999	−223.92351	0.86
CBS-COR-MP2	−0.42867	−0.37162	−0.83100	
CBS-COR-CCSD(T)	−0.41166	−0.40606	−0.84184	
CBS-MP2	−146.25054	−78.44161	−224.75451	1.70
CBS-CCSD(T)	−146.23353	−78.47604	−224.76535	1.52
ZPE from MP2 Hessian		0.05188	0.05411	
CBS CCSD(T) with ZPE	−146.23353	−78.42416	−224.71124	1.46
experiment[b]				1.40 ± 0.13
density functional theory[b]				1.41

[a] DZ, TZ, and QZ are the cc-pVXZ basis sets; CBS refers to complete basis set limit. [b] Values from ref 1.

TABLE 2: $Ag(C_2H_4)_2^+$ System: Total Energies (hartrees) and Binding Energies (eV)[a]

	total energies			
	C_2H_4	$Ag(C_2H_4)^+$	$Ag(C_2H_4)_2^+$	E_B (eV)
DZ-HF	−78.03968	−223.89183	−301.95853	0.74
DZ-MP2	−78.31504	−224.45326	−302.82303	1.49
DZ-CCSD(T)	−78.35513	−224.48018	−302.88368	1.32
TZ-HF	−78.06320	−223.91651	−302.00675	0.74
TZ-MP2	−78.39914	−224.64032	−303.09813	1.60
TZ-CCSD(T)	−78.43877	−224.65970	−303.14947	1.39
QZ-HF	−78.06846	−223.92196	−302.01717	0.73
QZ-MP2	−78.42503	−224.70774	−303.19288	1.64
QZ-CCSD(T)	−78.46166	−224.72218	−303.23605	1.42
CBS-HF	−78.06999	−223.92351	−302.02004	0.72
CBS-COR-MP2	−0.37162	−0.83100	−1.23726	
CBS-COR-CCSD(T)	−0.40606	−0.84184	−1.27445	
CBS-MP2	−78.44161	−224.75451	−303.25730	1.66
CBS-CCSD(T)	−78.47604	−224.76535	−303.29449	1.44
ZPE from MP2 Hessian	0.05188	0.05411	0.10854	
CBS CCSD(T) with ZPE	−78.42416	−224.71124	−303.18595	1.38
experiment[b]				1.31 ± 0.06
density functional theory[b]				1.20

[a] DZ, TZ, and QZ are the cc-pVXZ basis sets; CBS refers to complete basis set limit. [b] Values from ref 1.

co-workers. These final energies were obtained at both the MP2 and coupled cluster levels of theory. The coupled cluster method with single and double excitations augmented by perturbative triple excitations (CCSD(T)) was used. The core electrons are described by the Ag and Au ECPs, developed by Figgen et al.[16] As for the SBKJC ECP, these ECPs include 19 explicit electrons in the Ag or Au atom. Of these 19 electrons, 11 valence electrons are correlated, leaving 8 semicore electrons uncorrelated.

Using the improved Ag and Au basis sets, the binding energies (eq 1) of the $Ag(C_2H_4)_n^+$ and $Au(C_2H_4)_n^+$ systems were calculated at the Hartree−Fock,[17] MP2,[13] and CCSD(T)[18] levels of theory. The binding energies were calculated as $E_B(M) = E[M^+(C_2H_4)_{n-1}] + E[C_2H_4] - E[M^+(C_2H_4)_n]$, where M = Ag or Au. Since the cc-pVXZ basis sets improve systematically as the X increases from 2 to 4, the final binding energy was determined by extrapolation to the complete basis set (CBS) limit.[5] It has been shown[19] that the HF CBS limit is best found by a first-order exponential fit of the double, triple, and quadruple-ζ basis set data points. Correlation energy, obtained by using either MP2 or CCSD(T), was independently extrapo-

TABLE 3: $Ag(C_2H_4)_3^+$ System: Total Energies (hartrees) and Binding Energies (eV)[a]

	total energies			
	C_2H_4	$Ag(C_2H_4)_2^+$	$Ag(C_2H_4)_3^+$	E_B (eV)
DZ-HF	−78.03968	−301.95853	−380.00346	0.14
DZ-MP2	−78.31504	−302.82303	−381.16889	0.84
DZ-CCSD(T)	−78.35513	−302.88368	−381.26301	0.66
TZ-HF	−78.06320	−302.00675	−380.07412	0.11
TZ-MP2	−78.39914	−303.09813	−381.53117	0.92
TZ-CCSD(T)	−78.43877	−303.14947	−381.61459	0.72
QZ-HF	−78.06846	−302.01717	−380.08968	0.11
QZ-MP2	−78.42503	−303.19288	−381.65278	0.95
QZ-CCSD(T)	−78.46166	−303.23605	−381.72504	0.74
CBS-HF	−78.06999	−302.02004	−380.09407	0.11
CBS-COR-MP2	−0.37162	−1.23726	−1.64050	
CBS-COR-CCSD(T)	−0.40606	−1.27445	−1.70461	
CBS-MP2	−78.44161	−303.25730	−381.73457	0.97
CBS-CCSD(T)	−78.47604	−303.29449	−381.79868	0.77
ZPE from MP2 Hessian	0.05188	0.10854	0.16309	
CBS CCSD(T) with ZPE	−78.42416	−303.18595	−381.63559	0.69
experiment[b]				0.59 ± 0.03
density functional theory[b]				0.45

[a] DZ, TZ, and QZ are the cc-pVXZ basis sets; CBS refers to complete basis set limit. [b] Value from ref 1.

TABLE 4: $Au(C_2H_4)^+$ System: Total Energies (hartrees) and Binding Energies (eV)[a]

	total energies			
	Au^+	C_2H_4	$Au(C_2H_4)^+$	E_B (eV)
DZ-HF	−134.49840	−78.03968	−212.5864	1.31
DZ-MP2	−134.75129	−78.31504	−213.17013	2.82
DZ-CCSD(T)	−134.74461	−78.35513	−213.19014	2.46
TZ-HF	−134.49946	−78.0632	−212.61200	1.34
TZ-MP2	−134.83069	−78.39914	−213.34025	3
TZ-CCSD(T)	−134.82037	−78.43877	−213.35508	2.61
QZ-HF	−134.49951	−78.06846	−212.61753	1.35
QZ-MP2	−134.86332	−78.42503	−213.40102	3.07
QZ-CCSD(T)	−134.85156	−78.46166	−213.41134	2.67
CBS-HF	−134.49952	−78.06999	−212.61905	1.35
CBS-COR-MP2	−0.38758	−0.37162	−0.82380	
CBS-COR-CCSD(T)	−0.37477	−0.40606	−0.83085	
CBS-MP2	−134.88709	−78.44161	−13.44285	3.11
CBS-CCSD(T)	−134.87428	−78.47604	−213.44989	2.71
ZPE from MP2 Hessian		0.05188	0.05513	
CBS CCSD(T) with ZPE	−134.87428	−78.42416	−213.39477	2.62

[a] DZ, TZ, and QZ are the cc-pVXZ basis sets; CBS refers to complete basis set limit.

lated to the CBS limit by using an inverse cubic fit of the triple and quadruple-ζ data points.[20] Thus the CBS correlation energy was added to the HF energy giving the total energy. Tables 1−6 summarize the individual CBS energies and CBS binding energies.

Mulliken population analyses were obtained for each molecule by using the cc-pVTZ (C,H) and cc-pVTZ-PP (Ag, Au) basis sets. The populations were determined by using both HF and MP2 densities to qualitatively reveal how the electron density shifts upon addition of ethene ligands to the metal center. Tables 7−10 show the results of these analyses.

The reduced variational space (RVS) SCF[21,22] analysis was employed in order to examine the Ag^+−alkene bond. The RVS analysis describes the total interaction energy by decomposing the total Hartree−Fock interaction energy into contributions from electrostatic/exchange repulsion (CEX), polarization (POL), charge transfer (CT), and residual (RES) terms:

$$E_{INT} = E_{CEX} + E_{POL} + E_{CT} + E_{RES} \quad (2)$$

For the purpose of this analysis, the cc-pVDZ basis set for carbon and hydrogen, and the cc-pVDZ-PP basis set for silver were employed. Since this analysis was performed at the Hartree−Fock level of theory, it must be viewed as qualitative.

Additionally, multiconfiguration self-consistent field (MCSCF) wave functions, using an active space of two electrons in

TABLE 5: $Au(C_2H_4)_2^+$ System: Total Energies (hartrees) and Binding Energies (eV)[a]

	total energies			
	C_2H_4	$Au(C_2H_4)^+$	$Au(C_2H_4)_2^+$	E_B (eV)
DZ-HF	−78.03968	−212.58640	−290.67842	1.42
DZ-MP2	−78.31504	−213.17013	−291.57133	2.34
DZ-CCSD(T)	−78.35513	−213.19014	−291.62000	2.03
TZ-HF	−78.06320	−212.61200	−290.72845	1.45
TZ-MP2	−78.39914	−213.34025	−291.82951	2.45
TZ-CCSD(T)	−78.43877	−213.35508	−291.87182	2.12
QZ-HF	−78.06846	−212.61753	−290.73916	1.45
QZ-MP2	−78.42503	−213.40102	−291.91777	2.50
QZ-CCSD(T)	−78.46166	−213.41134	−291.95261	2.17
CBS-HF	−78.06999	−212.61905	−290.74207	1.44
CBS-COR-MP2	−0.37162	−0.82380	−1.23519	
CBS-COR-CCSD(T)	−0.40606	−0.83085	−1.26459	
CBS-MP2	−78.44161	−213.44285	−291.97726	2.53
CBS-CCSD(T)	−78.47604	−213.44989	−292.00666	2.20
ZPE from MP2 Hessian	0.05188	0.05513	0.11015	
CBS CCSD(T) with ZPE	−78.42416	−213.39477	−291.89651	2.11

[a] DZ, TZ, and QZ are the cc-pVXZ basis sets; CBS refers to complete basis set limit.

TABLE 6: $Au(C_2H_4)_3^+$ System: Total Energies (hartrees) and Binding Energies (eV)[a]

	total energies			
	C_2H_4	$Au(C_2H_4)_2^+$	$Au(C_2H_4)_3^+$	E_B (eV)
DZ-HF	−78.03968	−290.67842	−368.71698	−0.03
DZ-MP2	−78.31504	−291.57133	−369.92380	1.02
DZ-CCSD(T)	−78.35513	−291.62000	−369.99929	0.66
TZ-HF	−78.06320	−290.72845	−368.78958	−0.06
TZ-MP2	−78.39914	−291.82951	−370.26925	1.10
TZ-CCSD(T)	−78.43877	−291.87182	−370.33738	0.73
QZ-HF	−78.06846	−290.73916	−368.80532	−0.06
QZ-MP2	−78.42503	−291.91777	−370.38493	1.15
QZ-CCSD(T)	−78.46166	−291.95261	−370.44266	0.77
CBS-HF	−78.06999	−290.74207	−368.80968	−0.06
CBS-COR-MP2	−0.37162	−1.23519	−1.65253	
CBS-COR-CCSD(T)	−0.40606	−1.26459	−1.70267	
CBS-MP2	−78.44161	−291.97726	−370.46221	1.18
CBS-CCSD(T)	−78.47604	−292.00666	−370.51235	0.81
ZPE from MP2 Hessian	0.05188	0.11015	0.16574	
CBS CCSD(T) with ZPE	−78.42416	−291.89651	−370.34662	0.71

[a] DZ, TZ, and QZ are the cc-pVXZ basis sets; CBS refers to complete basis set limit.

two orbitals (2,2), were obtained by using GAMESS for both ethene and $Au(C_2H_4)^+$, in order to examine the Au^+−ethene bond. The active space employed for ethene consists of the π and π^* orbitals. For $Au(C_2H_4)^+$ the corresponding two orbitals are HOMO and LUMO. The cc-pVTZ basis sets were used for C and H, while the spdsMCP[23] (model core potential)[24,25] basis set was used for Au^+. Table 13 gives the density of each orbital in the active space for both molecules.

Results and Discussion

The total and binding energies for the $Ag^+(C_2H_4)_n$ complexes are listed in Tables 1, 2, and 3, for $n = 1$, 2, and 3, respectively. In general, the binding energies predicted by MP2 are already too high when the cc-pVDZ basis set is used. As the basis set is improved, MP2 predicts larger binding energies, and therefore the agreement with the experimental value worsens. This tendency of MP2 to overbind has been reported previously.[5,26,27] On the other hand, CCSD(T) binding energies are too small with the smaller basis sets and therefore improve as the basis set improves. This means that extrapolation to the CBS limit worsens the predicted MP2 binding energies, but improves the predicted CCSD(T) binding energies. The uncorrected CCSD(T) CBS binding energy of Ag^+ to C_2H_4 is 1.52 eV (Table 1), compared with the experimental value of 1.40 ± 0.13 eV. Including vibrational zero point energy (ZPE) corrections reduces the predicted binding energy to 1.46 eV (Tables 1 and 11), in excellent agreement with experiment. Following a similar procedure, the calculated ZPE-corrected CCSD(T)/CBS binding

TABLE 7: HF Mulliken Population Analysis of $Ag(C_2H_4)_n^+$ Systems

molecule	unique atom	s	p	d	f	g	total	charge
C_2H_4	1 C	3.3016	2.8919	0.0825	0.0066	0.0000	6.2826	−0.2826
	3 H	0.8317	0.0249	0.0021	0.0000	0.0000	0.8587	0.1413
Ag^+	1 Ag	2.0000	6.0000	10.0000	0.0000	0.0000	18.0000	1.0000
$Ag(C_2H_4)^+$	1 Ag	2.2701	6.1259	9.9486	0.0016	0.0000	18.3463	0.6538
	2 C	3.3096	2.8452	0.0944	0.0058	0.0000	6.2550	−0.2550
	4 H	0.7541	0.0297	0.0021	0.0000	0.0000	0.7859	0.2141
$Ag(C_2H_4)_2^+$	1 Ag	2.5228	6.1873	9.9078	0.0030	0.0000	18.6208	0.3792
	2 C	3.3126	2.8424	0.0943	0.0059	0.0000	6.2553	−0.2553
	4 C	3.3126	2.8424	0.0943	0.0059	0.0000	6.2553	−0.2553
	6 H	0.7640	0.0286	0.0021	0.0000	0.0000	0.7948	0.2052
	10 H	0.7640	0.0286	0.0021	0.0000	0.0000	0.7948	0.2052
$Ag(C_2H_4)_3^+$	1 Ag	2.4795	6.3549	9.8745	0.0038	0.0000	18.7128	0.2872
	2 C	3.2965	2.8792	0.0940	0.0060	0.0000	6.2758	−0.2758
	4 C	3.2967	2.8791	0.0940	0.0060	0.0000	6.2758	−0.2758
	6 C	3.2964	2.8792	0.0940	0.0060	0.0000	6.2757	−0.2757
	8 H	0.7725	0.0281	0.0021	0.0000	0.0000	0.8027	0.1973
	12 H	0.7726	0.0281	0.0021	0.0000	0.0000	0.8028	0.1973
	16 H	0.7726	0.0281	0.0021	0.0000	0.0000	0.8027	0.1973

TABLE 8: HF Mulliken Population Analysis of $Au(C_2H_4)_n^+$ System

molecule	unique atom	s	p	d	f	g	total	charge
C_2H_4	1 C	3.3016	2.8919	0.0825	0.0066	0.0000	6.2826	−0.2826
	3 H	0.8317	0.0249	0.0021	0.0000	0.0000	0.8587	0.1413
Au^+	1 Au	2.0000	6.0000	10.0000	0.0000	0.0000	18.0000	1.0000
$Au(C_2H_4)^+$	1 Au	2.6431	6.1512	9.7353	0.0096	0.0003	18.5395	0.4605
	2 C	3.2531	2.7874	0.0999	0.0070	0.0000	6.1473	−0.1473
	4 H	0.7562	0.0331	0.0022	0.0000	0.0000	0.7915	0.2086
$Au(C_2H_4)_2^+$	1 Au	2.9099	6.3460	9.6065	0.0165	0.0003	18.8793	0.1208
	2 C	3.2643	2.8079	0.0991	0.0066	0.0000	6.1779	−0.1779
	4 C	3.2643	2.8079	0.0991	0.0066	0.0000	6.1779	−0.1779
	6 H	0.7674	0.0316	0.0022	0.0000	0.0000	0.8012	0.1988
	10 H	0.7674	0.0316	0.0022	0.0000	0.0000	0.8012	0.1988
$Au(C_2H_4)_3^+$	1 Au	2.8036	6.6828	9.4979	0.0213	0.0003	19.0059	−0.0059
	2 C	3.2515	2.8547	0.1004	0.0065	0.0000	6.2132	−0.2132
	4 C	3.2517	2.8548	0.1004	0.0065	0.0000	6.2133	−0.2133
	6 C	3.2516	2.8548	0.1004	0.0065	0.0000	6.2133	−0.2133
	8 H	0.7768	0.0306	0.0022	0.0000	0.0000	0.8096	0.1904
	12 H	0.7768	0.0306	0.0022	0.0000	0.0000	0.8095	0.1905
	16 H	0.7768	0.0306	0.0022	0.0000	0.0000	0.8096	0.1905

energies for $n = 2$, 3 (Tables 2 and 3, respectively, Table 11) are 1.38 and 0.69 eV, respectively, compared with the experimental values of 1.31 ± 0.06 and 0.59 ± 0.03, respectively. So, the CCSD(T)/CBS predicted binding energy for $n = 2$ is just slightly outside the experimental error bars, while that for $n = 3$ is a little too high. Such good agreement reveals the importance of having systematic high quality basis sets for the heavy elements. It is interesting that the differential binding energy decreases as one goes from $n = 1$ to $n = 2$ and decreases significantly from $n = 2$ to $n = 3$.

Experimental binding energies for $Au(C_2H_4)_n^+$ are not available. However, one expects similar trends to those found for the Ag^+ system, that is, MP2/CBS binding energies that are too high relative to experiment and CCSD(T)/CBS binding energies that are in good agreement with experiment. The calculated binding energies of Au^+ to ethene are listed in Tables 4−6 for $n = 1-3$, respectively. As noted in the previous study of propene,[5] Au^+ binds to ethene more strongly than does Ag^+: for $n = 1$, 2.62 vs 1.46 eV at the CCSD(T)/CBS level of theory. However, the binding of ethene to Au^+ decreases more rapidly as n increases. The CCSD(T)/CBS binding energies of the $M(C_2H_4)_3^+$ (M = Ag, Au) complexes differ by only a predicted 0.02 eV. The binding energies of both Ag^+ and Au^+ to ethene follow the same trend: a small decrease in the differential binding energy on going from $n = 1$ to $n = 2$, followed by a much larger decrease from $n = 2$ to $n = 3$. This suggests that the binding of the metal to the first two ethenes has some covalent character, while the binding of the third ligand is primarily electrostatic.

The essential features of the optimized geometries for the Ag^+ and Au^+ complexes are shown in Figure 1. The geometries of the $M^+(C_2H_4)$ complexes resemble a T shape. Upon complexation with a second ligand, both the silver and gold complexes have a staggered arrangement of the two ethenes relative to each other. This structure is lower in energy than the eclipsed geometry. In all of the complexes, the C−C double bond is longer than its length of 1.339 Å in the isolated molecule.[28] For Ag^+ complexes this CC bond distance increase

TABLE 9: MP2 Mulliken Population Analysis of $Ag(C_2H_4)_n^+$ System

molecule	unique atom	s	p	d	f	g	Total	Charge
C_2H_4	1 C	3.3093	2.8878	0.0930	0.0097	0.0000	6.2997	−0.2997
	3 H	0.8201	0.0273	0.0027	0.0000	0.0000	0.8501	0.1499
Ag^+	1 Ag	2.0024	6.0104	9.9035	0.0800	0.0037	18.0000	1.0000
$Ag(C_2H_4)^+$	1 Ag	2.3234	6.1367	9.8270	0.0853	0.0038	18.3762	0.6238
	2 C	3.3187	2.8337	0.1078	0.0092	0.0000	6.2693	−0.2693
	4 H	0.7382	0.0305	0.0027	0.0000	0.0000	0.7713	0.2287
$Ag(C_2H_4)_2^+$	1 Ag	2.6007	6.2186	9.7612	0.0894	0.0039	18.6739	0.3261
	2 C	3.3224	2.8335	0.1076	0.0093	0.0000	6.2728	−0.2728
	4 C	3.3224	2.8335	0.1076	0.0093	0.0000	6.2728	−0.2728
	6 H	0.7471	0.0295	0.0027	0.0000	0.0000	0.7794	0.2206
	10 H	0.7471	0.0295	0.0027	0.0000	0.0000	0.7794	0.2206
$Ag(C_2H_4)_3^+$	1 Ag	2.5642	6.3976	9.7091	0.0914	0.0040	18.7662	0.2338
	2 C	3.3060	2.8729	0.1079	0.0093	0.0000	6.2960	−0.2960
	4 C	3.3061	2.8729	0.1078	0.0093	0.0000	6.2961	−0.2961
	6 C	3.3058	2.8729	0.1079	0.0093	0.0000	6.2959	−0.2959
	8 H	0.7561	0.0293	0.0027	0.0000	0.0000	0.7881	0.2119
	12 H	0.7561	0.0293	0.0027	0.0000	0.0000	0.7882	0.2118
	16 H	0.7561	0.0293	0.0027	0.0000	0.0000	0.7881	0.2119

TABLE 10: MP2 Mulliken Population Analysis of $Au(C_2H_4)_n^+$ System

molecule	unique atom	s	p	d	f	g	Total	Charge
C_2H_4	1 C	3.3093	2.8878	0.0930	0.0097	0.0000	6.2997	−0.2997
	3 H	0.8201	0.0273	0.0027	0.0000	0.0000	0.8501	0.1499
Au^+	1 Au	2.0052	6.0186	9.8818	0.0885	0.0060	18.0000	1.0000
$Au(C_2H_4)^+$	1 Au	2.7678	6.1507	9.5368	0.1070	0.0064	18.5688	0.4312
	2 C	3.2643	2.7748	0.1176	0.0106	0.0000	6.1672	−0.1672
	4 H	0.7379	0.0335	0.0028	0.0000	0.0000	0.7742	0.2258
$Au(C_2H_4)_2^+$	1 Au	2.9985	6.3740	9.4088	0.1179	0.0066	18.9057	0.0943
	2 C	3.2757	2.8040	0.1140	0.0100	0.0000	6.2037	−0.2037
	4 C	3.2757	2.8040	0.1140	0.0100	0.0000	6.2037	−0.2037
	6 H	0.7498	0.0323	0.0028	0.0000	0.0000	0.7850	0.2151
	10 H	0.7498	0.0323	0.0028	0.0000	0.0000	0.7850	0.2151
$Au(C_2H_4)_3^+$	1 Au	2.8987	6.6903	9.2978	0.1236	0.0068	19.0171	−0.0171
	2 C	3.2622	2.8543	0.1167	0.0100	0.0000	6.2431	−0.2431
	4 C	3.2624	2.8543	0.1167	0.0100	0.0000	6.2433	−0.2433
	6 C	3.2623	2.8543	0.1167	0.0100	0.0000	6.2432	−0.2432
	8 H	0.7591	0.0318	0.0028	0.0000	0.0000	0.7936	0.2064
	12 H	0.7591	0.0318	0.0028	0.0000	0.0000	0.7936	0.2064
	16 H	0.7591	0.0318	0.0028	0.0000	0.0000	0.7936	0.2064

TABLE 11: Summary of Experimental and Calculated E_B Values (eV)

	$Ag(C_2H_4)_n^+$			$Au(C_2H_4)_n^+$ calculated
		calculated		
n	Experimental[a]	DFT[a]	CBS, CCSD(T)	CBS, CCSD(T)
1	1.40 ± 0.13	1.41	1.46	2.62
2	1.31 ± 0.06	1.20	1.38	2.11
3	0.59 ± 0.03	0.45	0.69	0.71

[a] Values from ref 1.

is approximately 0.02 Å, but hardly changes with the number of attached ligands. In the Au^+ complexes, the CC bonds are considerably longer, reflecting the stronger Au−ethene interactions in these complexes, and again suggesting some covalent character in the bonds to the first two ligands. The CC bond distances for $n = 2, 3$ are shorter than that for $n = 1$, reflecting the overall weaker average binding for larger values of n.

Mulliken population analyses (see Tables 7−10) with HF and MP2 densities result in similar trends. The main difference is that the MP2 populations exhibit a more pronounced electron density shift. As n increases for $M(C_2H_4)_n^+$, the Mulliken charge on the silver ion steadily decreases from +1. There is significant electron density shift into the higher energy empty 5s- and 5p-orbitals on M^+ as ligands are added. While the electron density shift to higher, empty s-orbitals is not unusual, it is interesting that the higher energy p-orbitals gain electron density as well. So, the charge on Ag^+ and Au^+ becomes delocalized on the ethenes upon complexation. This delocalization increases as more ligands are added.

The Ag^+−ethene bond distance varies only slightly with the number of ligands attached. For the Au^+ complexes the Au^+−CC bond midpoint distance steadily increases from 2.021 Å for $n = 1$ to 2.157 Å for $n = 3$ (see Figure 1). Even though Au is below Ag in the Periodic Table, the Au−ethene distances are shorter, reflecting in part the stronger binding for Au^+. Au^+ exhibits the same trends in Mulliken populations as Ag^+, but,

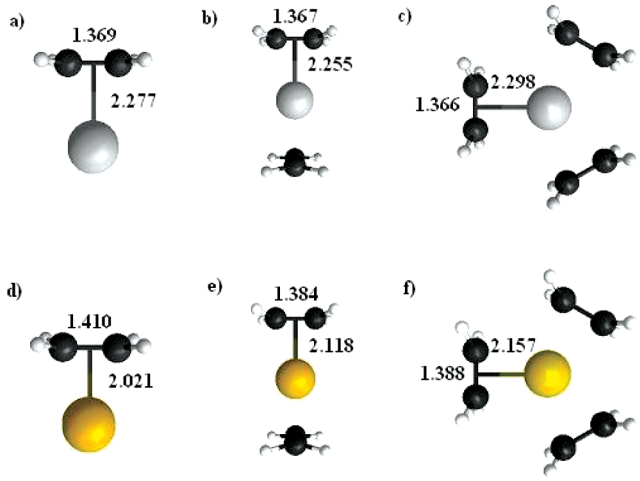

Figure 1. Predicted geometries of (a) $Ag(C_2H_4)^+$, (b) $Ag(C_2H_4)_2^+$, (c) $Ag(C_2H_4)_3^+$, (d) $Au(C_2H_4)^+$, (e) $Au(C_2H_4)_2^+$, and (f) $Ag(C_2H_4)_3^+$. All bond lengths are in Å. The M^+−ethene bond is measured from the metal ion to the midpoint of the C−C double bond.

TABLE 12: Summary of Reduced Variational Space (RVS) Analysis

	energy (kcal/mol)		
interaction type	$Ag(C_2H_4)^+$	$Ag(C_2H_4)_2^+$	$Ag(C_2H_4)_3^+$
Coulomb/electrostatic (ES)	−41.43	−86.37	−118.26
exchange repulsion (EX)	52.12	112.38	152.35
total Coulomb/exchange (CEX)	10.69	26.01	34.09
polarization (POL)	−10.99	−23.21	−29.75
charge transfer (CT)	−19.39	−39.18	−45.53
total interaction energy	−22.57	−41.84	−48.38
BSSE[a] corrected total interaction energy	−21.91	−40.50	−46.28
differential binding energy	−21.91	−18.59	−5.78

[a] Basis set superposition error.

as illustrated in Tables 9 and 10, Au^+ has a greater overall electron density shift, which also indicates a stronger interaction with the ligands. For $n = 3$, the Ag^+ and Au^+ distances approach each other, following the trends of the differential binding energies. The previous density functional theory study of the Ag system by Manard et al.[1] predicts rather larger Ag^+−ethene distances. The predicted MP2 Ag^+−ethene bond distances are 0.07−0.15 Å shorter than those predicted by DFT. It may be that the MP2 distances are too short, given the tendency of this method to overbind.[5,26,27]

Table 12 illustrates the RVS energy decomposition for the three Ag^+ species. For all three Ag^+ complexes, the electrostatic, polarization, and charge transfer contributions are stabilizing (attractive), whereas the uniquely quantum mechanical exchange repulsion is destabilizing. The electrostatic contribution is the largest attractive term, as one would expect, followed by charge transfer and then polarization.

The charge transfer contribution to bonding is the basis for the Dewar−Chatt−Duncanson (DCD) model of transition metal−alkene bonding.[29] So, it is interesting to decompose the interaction energy by using the RVS analysis. As shown in Table 12, charge transfer plays a significant, but not primary, role in Ag^+−C_2H_4 bonding. The most important contribution to the binding clearly arises from electrostatics. The DCD model assumes that electron density from the ethene π bond is donated to an empty orbital of appropriate symmetry on the metal center. This notion is consistent with the charge delocalization discussed earlier. Back-donation, according to this model, also occurs from the metal filled d-orbitals into the unoccupied antibonding π^* molecular orbital on ethene.[26] The geometry of the complexes does provide some evidence for the DCD model. Upon complexation with Ag^+, the C−C double bond lengthens by 0.02 Å, suggesting the possibility of some back-donation from Ag^+ filled 4d orbitals into the unoccupied π^* orbital of ethene. When a complex with Au^+ is formed, the double bond lengthens by 0.04−0.07 Å, again suggestive of even more back-bonding.

TABLE 13: Electron Density of π and π^* Orbitals from (2,2) MCSCF Calculation

	ethene	$Au(C_2H_4)^+$	difference
π	1.9126743	1.9512156	0.0385413
π^*	0.0873257	0.0487844	−0.0385413

MCSCF calculations can be employed to assess the electron density in antibonding orbitals. This is illustrated in Table 13, where the electron densities in the π and π^* orbitals are shown for the $Au(C_2H_4)^+$ complex. This species was chosen for analysis because it exhibits the largest binding energy. One would therefore expect the largest electron density shift. Nonetheless, as seen in the table, upon complexation, electron density is actually reduced in the π^* orbital and increased in the π orbital, with a very small net charge transfer of 0.04 electron. There is, therefore, little evidence of back-bonding, in contrast to the expectation of the DCD model.

Of course, it is important to recognize that the charge transfer contribution to the binding energy will decrease as the size of the basis set increases.[30] In the CBS limit, the charge transfer contribution will become zero. So, it is likely that the binding in these complexes is largely driven by electrostatic interactions. Indeed, as shown in Table 12, the relative importance of the electrostatic contribution to the binding energy increases with the number of ligands. This is especially true on going from two to three ligands. The RVS and similar analyses do not account for covalent bonding (i.e., bonding that arises from the constructive interference of wave functions on combining species, such as a metal and ethane[31]). It is likely, based on the discussion in previous paragraphs, that covalent interactions play some role in the M^+−ethene binding.

Conclusions

By using the combination of coupled cluster theory and the systematic Ag and Au basis sets, the binding energies of Ag^+ and Au^+ with 1, 2, and 3 ethene molecules have been predicted. For Ag^+, this leads to excellent agreement with experiment. It is likely that the predicted binding energies for Au^+ will have a similar accuracy. While MP2 gives worsening agreement with experiment as the basis set progresses from DZ to QZ, the CCSD(T) agreement generally improves.

Gold ions bind more strongly than silver ions to ethene ligands. The experimentally observed binding pattern for Ag^+ of a small decrease in E_B when adding a second ligand and a larger decrease upon addition of a third ligand is reproduced for the Ag^+ system, and also predicted for the Au^+ system. Mulliken population analyses show that there is considerable electron density shift onto the metal ion as each ligand is added. Thus the positive charge is delocalized onto the ligands. Electrostatic interactions are the primary origin of bonding, according to a reduced variational space analysis, and it is likely that covalent interactions also play a role. Charge transfer and polarization interactions also play a role, but this role diminishes relative to the electrostatic contribution as the number of ligands increases.

Acknowledgment. The authors thank Dr. Ryan Olson for many helpful discussions. N.B. was supported in part by an Iowa State University Plagens Scholarship. This work was supported by a grant from the Air Force Office of Scientific Research.

References and Notes

(1) Manard, M. J.; Kemper, P. R.; Bowers, M. T. *Int. J. Mass Spectrom.* **2005**, *241*, 109.

(2) Chretien, S.; Gordon, M. S.; Metiu, H. *J. Chem. Phys.* **2004**, *121* (8), 3756.

(3) Manard, M. J.; Kemper, P. R.; Carpenter, C. J.; Bowers, M. T. *Int. J. Mass Spectrom.* **2005**, *241*, 99.

(4) Chretien, S.; Gordon, M. S.; Metiu, H. *J. Chem. Phys.* **2004**, *121* (20), 9925.

(5) Olson, R.; Varganov, S.; Gordon, M. S.; Metiu, H. *Chem. Phys. Lett.* **2005**, *412*, 416.

(6) Stephens, P. J.; Devlin, F. J.; Chabalowski, C. F.; Frisch, M. J. *J. Phys. Chem.* **1994**, *98*, 11623. Becke, A. D. *J. Chem. Phys.* **1993**, *98*, 5648. Becke, A. D. *Phys. Rev. A* **1988**, *38*, 3098.

(7) Francl, M. M.; Pietro, W. J.; Hehre, W. J.; Binkley, J. S.; Gordon, M. S.; Defrees, D. J.; Pople, J. A. *J. Chem. Phys.* **1982**, *77*, 3654. Clark, T.; Chandrasekhar, J.; Spitznagel, G. W.; Schleyer, P. V. *J. Comput. Chem.* **1983**, *4*, 294. Krishnan, R.; Binkley, J. S.; Seeger, R.; Pople, J. A. *J. Chem. Phys.* **1980**, *72*, 650. Gill, P. M. W.; Johnson, B. G.; Pople, J. A.; Frisch, M. J. *Chem. Phys. Lett.* **1992**, *197*, 499.

(8) Hay, P. J.; Wadt, W. R. *J. Chem. Phys.* **1985**, *82*, 270. Wadt, W. R.; Hay, P. J. *J. Chem. Phys.* **1985**, *82*, 284. Hay, P. J.; Wadt, W. R. *J. Chem. Phys.* **1985**, *82*, 299.

(9) Peterson, K. A.; Puzzarini, C. *Theor. Chem. Acc.* **2005**, *114*, 283.

(10) Schmidt, M. W.; Baldridge, K. K.; Boatz, J. A.; Elbert, S. T.; Gordon, M. S.; Jensen, J. H.; Koseki, S.; Matsunaga, N.; Nguyen, K. A.; Su, S.; Windus, T. L.; Dupuis, M.; Montgomery, J. A. *J. Comput. Chem.* **1993**, *12*, 1347. Piecuch, P.; Kucharski, S. A.; Knowalski, K.; Musia, M. *Comput. Phys. Commun.* **2002**, *149* (2), 71.

(11) Hehre, W. J.; Ditchfield, R.; Pople, J. A. *J. Phys. Chem.* **1972**, *56*, 2257. Hariharan, P. C.; Pople, J. A. *Theor. Chim. Acta* **1973**, *28*, 213.

(12) Stevens, W. J.; Krauss, M.; Basch, H.; Jasien, P. G. *Can. J. Chem.* **1992**, *70*, 612.

(13) Moller, C.; Plesset, M. S. *Phys. Rev.* **1934**, *46*, 618.

(14) Werner, H. J.; Knowles, P. J., *version 2002.6*. Amos, R. D.; Bernhardsson, A.; Berning, A.; Celani, P.; Cooper, D. L.; Deegan, M. J. O.; Dobbyn, A. J.; Eckert, F.; Hampel, C.; Hetzer, G.; Knowles, P. J.; Korona, T.; Lindh, R.; Lloyd, A. W.; McNicholas, S. J.; Manby, F. R.; Meyer, W.; Mura, M. E.; Nicklass, A.; Palmieri, P.; Pitzer, R.; Rauhut, G.; Schutz, M.; Schumann, U.; Stoll, H.; Stone, A. J.; Tarroni, R.; Thorsteinsson, T.; Werner, H. J. *MOLPRO*, a package of ab initio programs. Hampel, C.; Peterson, K.; Werner, H. J. *Chem. Phys. Lett.* **1992**, *190* (1). Deegan, M. J. O.; Knowles, P. J. *Chem. Phys. Lett.* **1994**, *227*, 321.

(15) Dunning, T. *J. Phys. Chem.* **1989**, *90*, 1007.

(16) Piggen, D.; Rauhut, G.; Dolg, M. *Chem. Phys.* **2005**, *311*, 227.

(17) Roothaan, C. C. J. *Rev. Mod. Phys.* **1951**, *23*, 69.

(18) Scuseria, G. E.; Lee, T. J. *J. Phys. Chem.* **1990**, *93*, 5851.

(19) Kutzelnigg, W. *Int. J. Quantum Chem.* **1994**, *51*, 447. Jensen, F. *Theor. Chem. Acc.* **2000**, *104*, 484.

(20) Kutzelnigg, W.; III, J. D. M. *J. Chem. Phys.* **1992**, *96*, 4484. Halkier, A.; Helgaker, T.; Jorgensen, P.; Klopper, W.; Koch, H.; Olsen, J.; Wilson, A. K. *Chem. Phys. Lett.* **1998**, *286*, 243. Bytautas, L.; Ruedenberg, K. *J. Chem. Phys.* **2005**, *122*, 154110.

(21) Stevens, W. J.; Fink, W. H. *Chem. Phys. Lett.* **1987**, *139*, 15.

(22) Chen, W.; Gordon, M. S. *J. Phys. Chem.* **1996**, *100*, 14316.

(23) Unpublished work by Hirotoshi Mori.

(24) Huzinaga, S. *Can. J. Chem.* **1995**, *73*, 619.

(25) Osanai, Y.; Soejima, E.; Noro, T.; Mori, H.; Mon, M. S.; Klobukowski, M.; Miyoshi, E. *Chem. Phys. Lett.* **2008**, *463*, 230.

(26) Varganov, S. A.; Olson, R. M.; Gordon, M. S.; Metiu, H. *J. Chem. Phys.* **2003**, *119*, 233.

(27) Varganov, S. A.; Olson, R. M.; Gordon, M. S.; Mills, G.; Metiu, J. *J. Chem. Phys.* **2004**, *120*, 5169.

(28) *CRC, Handbook of Chemistry and Physics*, 84th ed.; Lide, D., Ed.; CRC Press: Boca Raton, FL, 2003/04; pp 9−33.

(29) Frenking, G.; Frohlich, N. *Chem. Rev.* **2000**, *100*, 717.

(30) Li, H.; Gordon, M. S.; Jensen, J. H. *J. Phys. Chem.* **2006**, *124*, 1.

(31) Ruedenberg, K. *Rev. Mod. Phys.* **1962**, *34*, 326.

JP900372D